

available at www.sciencedirect.comjournal homepage: www.elsevier.com/locate/biochempharm

Modulation of mitochondrial metabolic function by phorbol 12-myristate 13-acetate through increased mitochondrial translocation of protein kinase C α in C2C12 myocytes

Ying Wang¹, Gopa Biswas, Subbuswamy K. Prabu, Narayan G. Avadhani*

Laboratories of Biochemistry, Department of Animal Biology and The Mari Lowe Center for Comparative Oncology, School of Veterinary Medicine, University of Pennsylvania, Philadelphia, PA 19104, United States

ARTICLE INFO

Article history:

Received 21 April 2006

Accepted 20 June 2006

Abbreviations:

CcO, cytochrome c oxidase

PDH, pyruvate dehydrogenase

PKC, protein kinase C

PMA, phorbol 12-myristate 13-acetate

ROS, reactive oxygen species

ABSTRACT

Protein kinase C (PKC) agonists including phorbol 12-myristate 13-acetate (PMA) not only induce the redistribution of cytosolic PKC to various subcellular compartments but also activate the kinase domain of the protein. In the present study we have investigated the nature of mitochondrial PKC pool and its effects on mitochondrial function in cells treated with PMA. Treatment of C2C12 myoblasts, C6 glioma and COS7 cells with PMA resulted in a dramatic redistribution of intracellular PKC α pool, with large fraction of the protein pool sequestered in the mitochondrial compartment. We also observed mitochondrial PKC δ accumulation in a cell restricted manner. The intramitochondrial localization was ascertained by using a combination of protection against protease treatment of isolated mitochondria and immunofluorescence microscopy. PMA-induced mitochondrial localization of PKC α was accompanied by increased mitochondrial PKC activity, altered cell morphology, disruption of mitochondrial membrane potential, decreased complex I and pyruvate dehydrogenase activities, and increased mitochondrial ROS production. All of these changes could be retarded by treatment with PKC inhibitors. These results show a direct role for PMA-mediated PKC α translocation to mitochondria in inducing mitochondrial toxicity.

© 2006 Elsevier Inc. All rights reserved.

1. Introduction

Protein kinase C is composed of a family of serine/threonine kinases that modulate a variety of physiological functions such as cell proliferation, differentiation and apoptosis. PKC isoforms are divided into three subgroups: (1) the conventional PKCs, namely α , β I, β II and γ isoforms that are activated by Ca²⁺, phosphatidylserine (PS) and diacylglycerol (DAG), or phorbol 12-myristate 13-acetate (PMA). (2) The novel PKC isoenzymes consisting of the PKC δ , ϵ , η , θ and μ , that are activated by PS and DAG or PMA but insensitive to Ca²⁺. (3) The atypical isoforms, ζ and ι/τ that are not affected

by Ca²⁺, DAG or PMA, but are dependent on PS for activation [1,2].

Protein kinase C isozymes are distributed throughout the cell with a distinct cell specific difference in the pattern of distribution. Additionally, the functional role of a specific PKC isoform can be different from one cell type to another. It is generally believed that PKCs exist in inactive state and are activated in response to specific stimuli. A key regulator of PKC function is thought to be its pattern of subcellular distribution upon stimulation, and the availability of appropriate substrates. Thus, translocation (redistribution) of PKC within intracellular compartments is an important indicator of its activation. In rat

* Corresponding author. Fax: +1 215 573 6651.

E-mail address: narayan@vet.upenn.edu (N.G. Avadhani).

¹ Present address: Department of Pathology, School of Medicine, University of Maryland, Baltimore, MD 21201, United States.

0006-2952/\$ – see front matter © 2006 Elsevier Inc. All rights reserved.

doi:10.1016/j.bcp.2006.06.032

skeletal myocytes, PMA and insulin induce tyrosine phosphorylation and translocation of PKC β II and δ to plasma membrane, which supports increased glucose uptake [3]. Physiological mitogens induce the nuclear translocation of PKC and the phosphorylation of nuclear lamine B by nuclear PKC β II, which is implicated in cell cycle control and mitosis [1]. Furthermore, the mode of activation of PKC may vary depending on the cell type, and stimulus, which make the function of PKC very complex. Reports show that the novel PKC forms such as PKC δ , ϵ but not the conventional PKC α , were activated upon mitogenic stimulation of quiescent rat 3Y1 fibroblasts [4]. Insulin is also known to induce the PKC δ translocation to plasma membrane in L6 cells [5] but not in 3T3-L1 adipocyte [6] although both cell lines are insulin-responsive.

The presence of PKC in the mitochondrial compartment has been known for some time [7], but its function remains unclear. A recent study showed that PMA-induced mitochondrial accumulation of PKC δ is associated with cytochrome c release and apoptosis in human U937 cells, thus suggesting a mitochondrial function for this isoform [8]. Since then, a number of studies showed that mitochondrial PKC δ , induced by different effectors is related to apoptosis in different cell lines [8,9]. It is known for some time that PKC ϵ plays important role in cardiac function, though the mechanism remained unclear until recent observations, which suggested that mitochondrial PKC ϵ and MAPK form signaling modules that are associated with cardioprotection [10]. The distribution of PKC α appears ubiquitous, but the effect of PKC α activation on mitochondrial function is paradoxical. In myeloid leukemia-derived HL60 cells, mitochondrial PKC α has been implicated in the suppression of apoptosis and resistance to chemotherapy [11] through phosphorylation of Bcl2. However, in renal cells, activated PKC α mediates mitochondrial dysfunction, decreased Na⁺ transport and cisplatin-induced apoptosis [12].

In the present study, we found that in C2C12 skeletal myocytes, COS7 and C6 glioma, PKC α is the major PKC subtype that is translocated to mitochondria when treated with PMA. PMA-induced mitochondrial translocation of PKC α caused disruption of mitochondrial transmembrane potential ($\Delta\psi$ m), decreased complex I activity, increased mitochondrial ROS production, and inhibition of PDH activity. Furthermore, PMA treatment and associated increase in mitochondrial PKC α activity caused a visible change in the morphology of C2C12 myocytes.

2. Materials and methods

2.1. Cell lines and culture

Murine C2C12 skeletal myoblast, C6 glioma, COS7 cells were grown in Dulbecco's minimum essential medium (DMEM) supplemented with 10% heat inactivated fetal calf serum, gentamycin 50 μ g/ml.

2.2. Cell fractionation and Western blot analysis

Mitochondria were isolated as described before [13]. Cells were homogenized in sucrose–mannitol buffer, 70 mM sucrose, 210 mM mannitol, 2 mM HEPES, 2 mM EDTA, pH 7.4, and 50 μ g

protease inhibitor (Roche Molecular Biochemicals, Indianapolis, IN, USA) in a Dounce homogenizer and fractionated into nuclear, post-mitochondrial and mitochondrial fractions. Resultant mitochondria were purified by sucrose density banding as described before [13]. Digestion of mitochondria with trypsin was carried out as described before [13]. Briefly, mitochondria (2.5 mg/ml) suspended in sucrose–mannitol buffer were treated with trypsin (100–300 μ g/ml) for 20 min on ice and the reaction was stopped by adding 300 μ g/ml of trypsin inhibitor. Mitochondria were re-isolated from trypsin-treated samples by sedimentation through 0.8 M sucrose and were washed twice with sucrose–mannitol buffer and mitochondrial proteins were analyzed by Western blot. Mitoplasts were prepared treating freshly isolated mitochondria with digitonin (Wako Chemicals, Richmond, VA) at a final concentration of 75 μ g/mg of protein, at 4 °C for 2 min and washed three times with the homogenization buffer [14]. Post-mitochondrial fraction was centrifuged at 100,000 $\times g$ for 1 h to get the cytosol (supernatant) and endoplasmic reticulum (pellet) fraction. Protein fractions solubilized in Laemmli's sample buffer were resolved on polyacrylamide gels and subjected to immunoblot analysis. Antibody for PKC α was purchased from BD transduction laboratories (Lexington, NY). Antibodies for PKC δ and β -tubulin from Santa Cruz Biotechnology (Santa Cruz, CA). Immunoblots were developed using the Pierce Super signal West Femto maximum sensitivity substrate kit (Pierce Biotechnology Inc., Rockford, IL) imaged and quantified in a Bio-Rad Fluor-S imaging system.

2.3. Immunofluorescence and light microscopy

C2C12 cells were grown on cover slips and treated with 100 nM PMA or DMSO as control. The cells were then processed for antibody staining essentially as described before [15] except that after permeabilization with 0.1% Triton X-100, cells were blocked with 5% goat serum for 1 h at room temperature. Cells were immunostained with 1:50 dilution of mouse antibody to the PKC α and 1:50 dilution of rabbit antibody to mitochondrial CcO I protein (Santa Cruz Biotechnology, Inc.) for 1 h at 37 °C. Cells were washed repeatedly with PBS, and sequentially incubated with Alexa 488-conjugated anti-mouse donkey IgG (Molecular Probes, Inc., Eugene, OR) for the detection of PKC α followed by Alexa 4594-conjugated anti-mouse goat IgG (Molecular Probes, Inc.) for the detection of CcO I for 1 h each at 37 °C at 1:100 dilution. Unbound secondary antibodies were removed by repeated washing with PBS. Fluorescence microscopy was carried out under a TCS laser scanning microscope (Leica Inc., Deerfield, IL).

For light microscopy cells grown on cover slips were treated with PMA (100 nM for 1 h). Control and treated cells were stained with hematoxylin/eosin (Fluka Biochemicals) for 20 min at room temperature, and washed three times with 1 \times PBS for 15 min each. The cover slips were mounted on slides using Permount mounting medium (Fisher Scientific) and viewed under bright field using Olympus BX61 microscope.

2.4. Measurement of mitochondrial membrane potential

Measurements were carried out spectrofluorometrically in cell suspension essentially as described before [15,16] with minor

modifications. Briefly, cells were harvested and washed with ice-cold extracellular medium (ECM) containing 120 mM NaCl, 5 mM KCl, 1 mM KH_2PO_4 , 0.2 mM MgCl_2 , 0.1 mM EGTA, 20 mM HEPES–Tris, pH 7.2. Non-permeabilized cells (1.2×10^6) were suspended in 1 ml intracellular medium (ICM) containing 20 mM HEPES–Tris pH 7.2, 120 mM NaCl, 5 mM KCl, 1 mM KH_2PO_4 . The membrane potential was measured as a function of mitochondrial uptake of MitoTracker Orange CM- H_2TMROS (50 nM) added to the cell suspension. Fluorescence was monitored in a multiwavelength-excitation dual wavelength-emission Delta RAM PTI spectrofluorometer at 525 nm excitation and 575 nm emission.

2.5. Assay for PKC activity

The PKC activity was measured using the PKC Assay System kit from Life Technologies (Grand Island, NY), which employs a PKC specific pseudosubstrate peptide inhibitor. The Ca^{2+} sensitive kinase activity was assayed by adding 5 mM EGTA to the assay mix, PKC enzyme was partially purified by chromatography on DEAE Sephacel microcolumns by a protocol described in the kit and assays were carried out in 50 μl volumes using 1 μCi of [^{32}P] ATP.

2.6. Enzyme assays for mitochondrial respiratory chain complexes

The activity of complex I (NADH:ubiquinone oxidoreductase), and complex II (succinate:ubiquinone oxidoreductase) activities were assayed as described [17]. Complex I specific activity was measured by following the decrease in absorbance due to the oxidation of NADH at 340 nm, with 425 nm as the reference wavelength ($\epsilon = 6.81 \text{ mM}^{-1} \text{ cm}^{-1}$). NADH (0.13 mM), ubiquinone 1 (65 μM) and antimycin A (2 $\mu\text{g}/\text{ml}$) were added to the assay medium and the absorbance change was recorded for 1–2 min. Mitochondria (50 μg) were added, and the NADH:ubiquinone oxidoreductase activity was measured for 3–5 min before adding rotenone (2 $\mu\text{g}/\text{ml}$), after which the activity was measured for an additional 3 min. Complex II activity was measured by following the reduction of 2,6-dichlorophenolindophenol at 600 nm ($\epsilon = 19.1 \text{ mM}^{-1} \text{ cm}^{-1}$). Mitochondria (50 μg) were pre-incubated in the assay medium (potassium phosphate, 25 mM, pH 7.2; MgCl_2 , 5 mM) plus succinate (20 mM) at 30 °C and the baseline rate was recorded for 3 min following the addition of antimycin A (2 $\mu\text{g}/\text{ml}$), rotenone (2 $\mu\text{g}/\text{ml}$), KCN (2 mM) and dichlorophenolindophenol (50 μM). The reaction was started by adding ubiquinone (65 μM), and the enzyme-catalyzed reduction of dichlorophenolindophenol was measured for 3–5 min. Complex II–III (succinic–cytochrome c reductase) was assayed as described by Tisdale [18]. Assays of enzymatic activity were carried out at 38 °C in a Beckman Model DU spectrophotometer equipped with a photomultiplier. The final reaction mixture contained 10 μM phosphate buffer, 1 μM NaN_3 , 0.2 μM EDTA, 5 mg BSA, 10 μM potassium succinate, pH 7.0, 0.3 M sucrose, 2 mM succinate and 50 μg mitochondrial protein and the assay mixture was pre-incubated for 2 min at 38 °C. The reaction was initiated by adding 1 mg ferricytochrome c and the change in absorbance was measured at 550 nm and followed at 10 s intervals over the first 2 min ($\epsilon = 18.5 \times 10^6 \text{ M}^{-1} \text{ cm}^{-1}$).

Cytochrome c activity (complex IV) was assayed spectrophotometrically by the method described by Smith [19], wherein the rate of oxidation of ferrocytochrome c was measured as decrease in absorbance at 550 nm. Assays were performed in 1 ml reaction volume containing 50 mM PO_4^{2-} (pH 7.0), 0.05% lauryl maltoside, 1 mM EDTA and 1–5 μg mitochondrial protein. The reaction was initiated by the addition of 80 μM ferrocytochrome c. Ferrocytochrome c concentrations were determined using an absorbance coefficient (reduced – oxidized) at 550 nm of $21.1 \text{ mM}^{-1} \text{ cm}^{-1}$. The COX activity is expressed in $\text{mol min}^{-1} \text{ mg protein}^{-1}$.

2.7. Assay of ROS production in isolated mitochondria

Mitochondrial ROS production was assayed as described before [20,21]. The lucigenin-enhanced chemiluminescence method was used by using Turner Designs TD-20/20 luminometer. Briefly, freshly isolated mitoplasts (100–200 μg protein) swollen by suspension in 10 mM potassium phosphate buffer (pH 7.8) was used in 200 μl assay system containing 0.5 mM NAD(P)H for the assay of ROS. Production of chemiluminescence was initiated by adding 5 μM lucigenin (N,N' -dimethyl-9,9'-biacridinium dinitrate, Sigma Chemical Co.) and light emission was recorded every 60 s for 5–10 min and was expressed as mean arbitrary luminiscence unit per min per mg protein [21].

ROS generation was also measured by a modified DCF-DA fluorescence method described before [20,21]. Stable non-fluorescent DCFH-DA (1 mM in methanol) was used in 1 ml assay mixture containing freshly isolated mitoplasts. DCFH-DA is hydrolyzed by cellular esterases to a non-fluorescent DCFH. Recent unpublished results show that mitochondria from various cells and tissues contain enzyme activity for the hydrolysis of DCFH-DA. DCFH is then rapidly oxidized by peroxy radicals to highly fluorescent DCF. In some cases, the ROS were also measured in presence of SOD (30 U/ml) or catalase (10 U/ml), both from Sigma, St. Louis, MO. The fluorescence was recorded in a Delta Ramp71 spectrofluorometer from Photon Technology International at an excitation 488 nm and emission 525 nm for 20 min.

2.8. Measurement of pyruvate dehydrogenase activity

The PDH activity was assayed by measuring the release of $^{14}\text{CO}_2$ from [$1\text{-}^{14}\text{C}$] pyruvic acid (PerkinElmer, Life Science) [22] in total assay volume of 125 μl using a final protein concentration of 90 $\mu\text{g}/\text{ml}$. For these assays, cells were incubated for 10 min at 37 °C in DMEM medium in the presence of 250 nM PMA. Cells were harvested in the 200 mM NaF, 10 mM dichloroacetic acid, 2 mM EDTA, 2 mM DTT, 0.2% Triton X-100 in 50 mM HEPES, pH 7.7. Incubations were carried out in tubes sealed with rubber caps that contained a center well (Kontes Glass Company, NJ). Enzyme was added to the assay medium (2 mM NAD^+ , 0.6 mM coenzyme A, 0.5 mM cocarboxylase, 1 mM DTT, 1 mM MgCl_2 , 0.1% Triton X-100, 200 mM Tris–HCl, pH 8.0) and preincubated for 4 min in 37 °C water bath. The assay was started by addition of pyruvate (100 μM pyruvate; 200,000 DPM [$1\text{-}^{14}\text{C}$]). Incubations were stopped with 0.4 ml 0.2 M H_2SO_4 , β -phenylethylamine (0.2 ml) was injected into the center well and

$^{14}\text{CO}_2$ collected for 90 min. Filters were removed and counted with scintillation fluid in Beckman Scintillation counter.

3. Results

3.1. Increased mitochondrial localization of PKC α in C2C12 cells in response to PMA treatment

Immunoblot analysis of soluble ($100,000 \times g$ supernatant) and membrane ($100,000 \times g$ pellet) fractions (Fig. 1A) showed that PKC α , δ , ϵ are the major PKC subtypes expressed in C2C12 cells. In unstimulated cells, PKC α and PKC δ were mostly in the cytosolic ($100,000 \times g$ supernatant) fraction while PKC ϵ was mostly in the membrane fraction. Furthermore, in unstimulated C2C12 cells, PKC α was mostly localized in the soluble cytosolic fraction with modest amount also detected in the mitochondrial fraction (Fig. 1B). However, in cells stimulated with 100 nM PMA for 2 h, the content of cytosolic PKC α was drastically reduced while that of ER, plasma membrane, nuclear and mitochondrial fractions was increased as shown before [23,24]. It should also be noted that in PMA stimulated cells, mitochondria were the predominant site of PKC α accumulation, only next to the plasma membrane fraction (Fig. 1B). In this study therefore, we focused our investigation on the mitochondrial levels of PKC α and δ isoforms in C2C12 myocytes and used C6 glioma and COS7 cells in limited number of experiments for comparison.

As shown in Fig. 2A, after PMA treatment, PKC α decreased rapidly in the cytosol with simultaneous increase in the mitochondrial fraction. In contrast, PMA had no detectable effect on the PKC δ level in the cytosol and mitochondria of C2C12 cells. The level of mitochondrial PKC α increased at 1 h

and peaked at 3 h of PMA treatment. At 6 h time point the mitochondrial level decreased substantially. This decrease may be due to the down-regulation since after 9 h, PKC α levels decreased to near control level in both mitochondria and the whole cell lysate (data not shown).

Experiments using different doses of PMA (0–250 nM) showed that at 10 nM concentration, the mitochondrial PKC α content increased only marginally (Fig. 2B). At 100 nM and 250 nM concentrations, however, a progressively increasing amount of PKC α was observed in the mitochondrial fraction (Fig. 1B). However, the mitochondrial PKC δ levels did not increase significantly by PMA treatment. The blots were co-developed with antibodies to tubulin and mitochondrial encoded CcO subunit I (CcO I) to assess the levels of proteins loaded on the gel. Furthermore, results show that the mitochondrial protein fraction interacted minimally with tubulin antibody, while the cytosolic protein did not show detectable interaction with CcO I antibody, indicating negligible cross-contamination. As seen from Fig. 2C, PMA treatment (100 nM for 1 h) also caused a change in the morphology of C2C12 myocytes. The treated cells were more elongated with pseudopodia-like membrane extensions.

To ascertain the intramitochondrial localization of PKC α in PMA-induced cells, we carried out a series of control experiments. In the first series, limited digestion with trypsin and also stripping of outermembrane by digitonin treatment were carried out. Immunoblot in Fig. 2D shows that cytosolic PKC α is highly sensitive to trypsin treatment. Mitochondrial PKC α was relatively resistant to digitonin treatment, which strips nearly 75% of the outermembrane under the conditions used, and also to digitonin + trypsin. Lysis of mitochondrial membrane with Triton-X100, on the other hand, rendered mitochondrial PKC α more sensitive to trypsin digestion. These

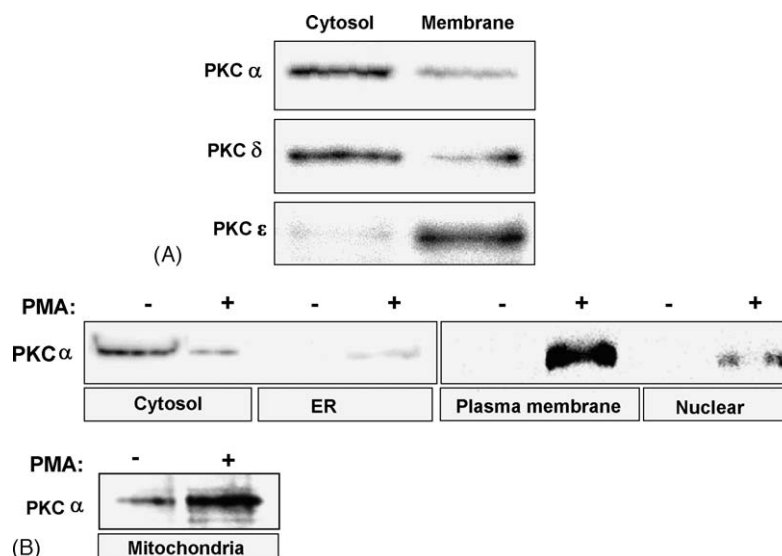


Fig. 1 – Detection of different PKC subtypes in the cytosolic and membrane fractions of C2C12 myocytes. (A) Total soluble ($100,000 \times g$ supernatant) and membrane ($100,000 \times g$ pellet) fractions (30 μg protein each) were subjected to immunoblot analysis using antibodies to PKC α , PKC δ and PKC ϵ as indicated. **(B)** Control C2C12 cells or cells treated with PMA (100 nM) for 2 h at 37 °C were fractionated into cytosol, ER, plasma membrane, nuclei and mitochondria using a standard procedure [44]. Protein fractions (30 μg each) were subjected to immunoblot analysis using antibody to PKC α . The immunoblots were developed using the Pierce Super signal West Femto substrate kit as described in Section 2 using antibodies to PKC α , PKC δ and PKC ϵ as indicated.

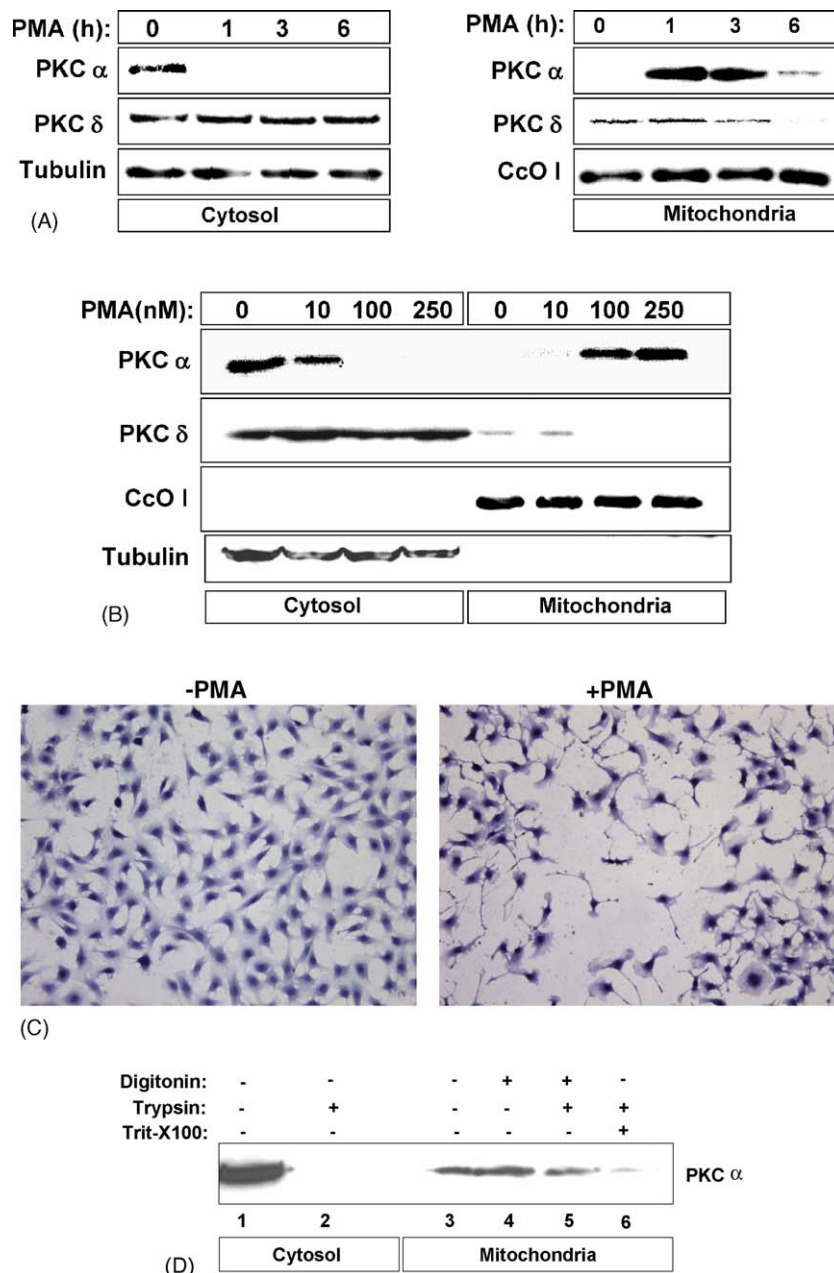


Fig. 2 – Increased mitochondrial PKC α content in response to PMA treatment. (A) C2C12 myoblasts were treated with 100 nM PMA for 0–6 h as indicated. Cytoplasmic (left panel) and mitochondrial (right panel) protein fractions (30 μ g each) were subjected to immunoblot analysis using anti-PKC α and PKC δ antibodies. (B) Cytosolic and mitochondrial protein fractions from C2C12 myocytes treated with increasing amounts of PMA (from 0 to 250 nM) were subjected to immunoblot analysis as in ‘A’. (C) Morphology of C2C12 myocytes treated with 100 nM PMA for 1 h. Control and treated cells were stained with hematoxylin/eosin (Fluka Biochemicals) and viewed under a bright field microscope (10 \times lense, Olympus BX61). (D) Intramitochondrial localization of PKC α was ascertained using trypsin and digitonin treatment. Mitochondria and cytosol from C2C12 cells treated with 100 nM PMA for 1 h were isolated in isolation buffer without added protease inhibitor. Freshly isolated mitochondria and cytosol were treated with trypsin (lanes 2, 5 and 6) and/or digitonin (lanes 4 and 5) as described in Section 2 and subjected to immunoblot analysis using PKC α antibody. In lane 6, mitochondria were treated with 0.1% Triton-X100 before adding trypsin. In ‘A’ and ‘B’, the blots were stripped and developed again with antibody to tubulin (cytosol) and antibody to CcO (mitochondria) to assess the level of protein loading.

results suggest that the PKC α subunit is indeed localized inside the mitochondrial innermembrane compartment.

In the second series of experiments, mitochondrial localization of PKC α was visualized by immunohistochemical

co-localization with mitochondria specific CcO (Fig. 3A). The PKC α specific staining in control cells showed a homogeneous staining suggesting a predominantly cytosolic distribution. In PMA treated cells, the PKC α stain was associated with

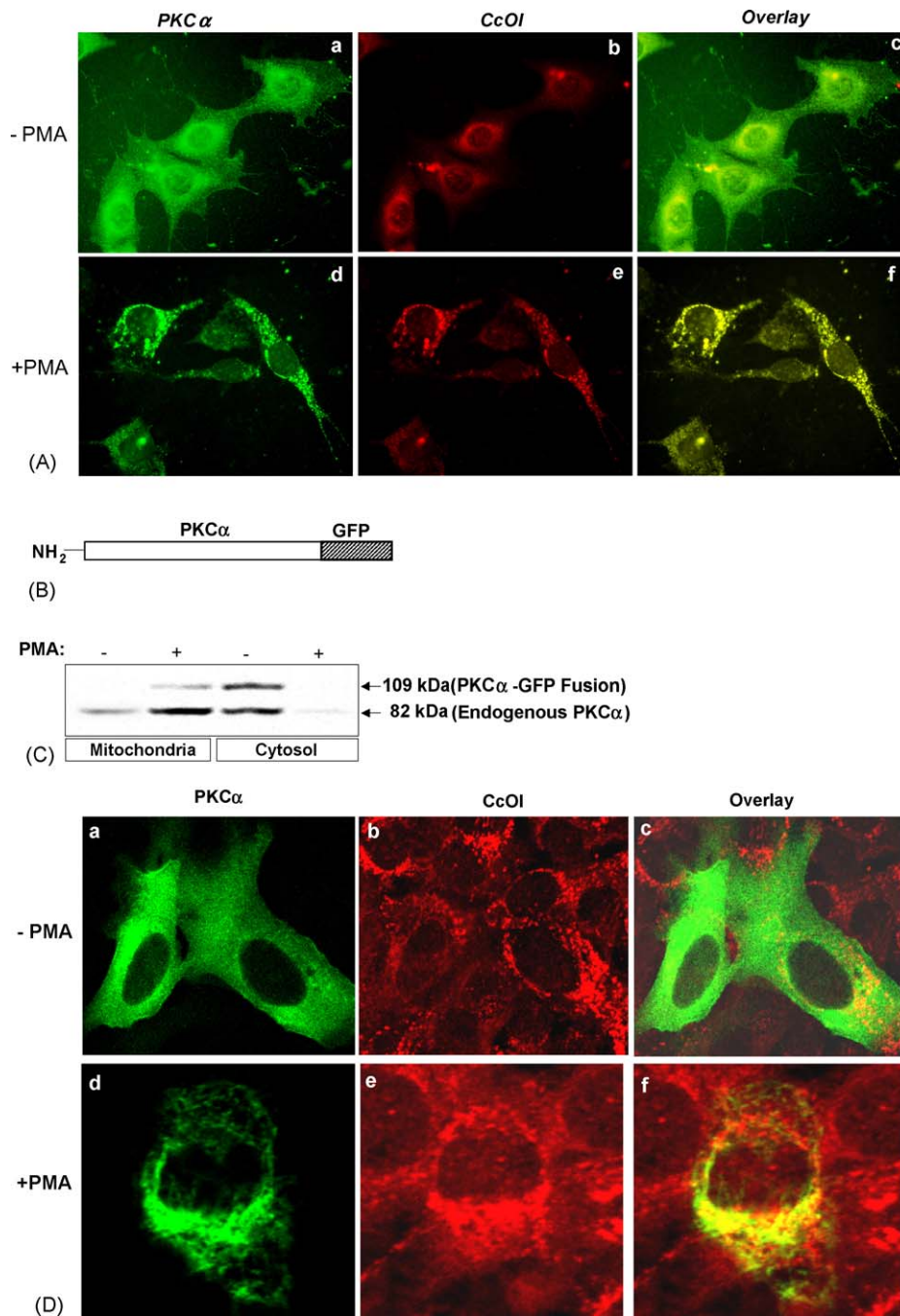


Fig. 3 – Mitochondrial localization of PKC α in response to PMA treatment. (A) C2C12 myocytes grown on cover slips were sequentially stained with mouse antibody to PKC α and Alexa 488 conjugated secondary antibody to mouse IgG (a and d) followed by mouse antibody to CcO I and Alexa 594 conjugated secondary antibody to mouse IgG as described in Section 2. PMA treatment (100 nM) was carried out for 1 h. Cells were subjected to confocal fluorescence microscopy. Images in c and f represent overlaid images of a and d with those in b and e, respectively. (B) A cartoon showing the map of the GFP fusion construct. (C) Immunoblot analysis of protein fractions from C2C12 cells stably transfected with GFP fusion cDNA construct with and without PMA treatment. The mitochondrial and cytosolic proteins (30 μ g each) were subjected to immunoblot analysis using PKC α antibody. (D) Immunofluorescence microscopy of C2C12 cells stably transfected with PKC α -GFP fusion cDNA construct. Stably transfected cells were sequentially stained with mouse antibody to CcO I and Alexa 594 conjugated anti-mouse IgG. Images in a and d represent green fluorescent images of control (-PMA) and PMA treated cells. Images in b and e represent patterns of CcO I antibody stained patterns. Images in c and f are overlaid images of a with b and d with e, respectively. Details of staining and microscopy were as described in 'A' above.

punctuate membranous structures, which co-localized with mitochondria-specific stain (CcO I antibody). These results provide further support for mitochondrial translocation of PKC α in cells treated with PMA (Fig. 3A). We also generated a PKC α -GFP fusion cDNA construct (see Fig. 3B) to study the intracellular distribution of PKC α in PMA treated C2C12 cells. C2C12 cells were transfected with the GFP-fusion construct and the mitochondrial and cytosolic proteins from PMA treated and untreated cells were subjected to immunoblot analysis with PKC α antibody. Immunoblot in Fig. 3C shows that both the ectopically expressed GFP-fusion protein (109 kDa) and the endogenous PKC α protein (82 kDa) are detected in the cytoplasmic fraction in cells not treated with PMA. In PMA-treated cells, however, the levels of antibody reactive proteins (both 82 kDa and 109 kDa) increased in the mitochondrial fraction. In Fig. 3D, cells transfected with the GFP-fusion cDNA construct, and treated with or without PMA, were stained with primary antibody to CcO I subunit and Alexa 594 conjugated secondary antibody, and subjected to fluorescence microscopy. It is seen that in control cells not treated with PMA, the green fluorescence was distributed uniformly throughout the cells suggesting mostly a cytosolic distribution. In these cells, a relatively small fraction of green fluorescence was co-localized with CcO I specific stain. In PMA treated cells, the green fluorescence was distributed in particulate membrane structures including punctuate structures, reminiscent of mitochondria. Substantial part of green fluorescence associated with the particulate structures co-localized with the CcO specific stain.

3.2. PMA-mediated mitochondrial translocation of PKC α and PKC δ in other cell lines

The generality of PKC subunit translocation to mitochondria in response to PMA treatment was investigated using C6 glioma and COS7 cells that are derived from different tissues, namely brain and kidney, respectively. Immunoblot in Fig. 4 shows that both in C6 glioma and COS 7 cells, the cytosolic PKC α contents were reduced after PMA treatment. As observed in C2C12 cells, the mitochondrial PKC α contents were markedly increased in cells treated with PMA. Nevertheless cell specific differences were observed in both the levels and size of mitochondrial PKC δ

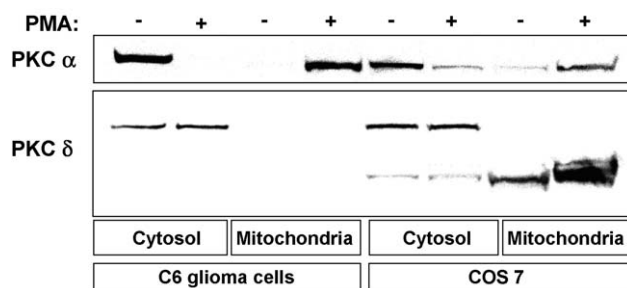


Fig. 4 – PMA-induced mitochondrial PKC α and PKC δ proteins in C6 glioma and COS7 cells. Mitochondrial and cytosolic protein fractions from control and PMA treated (100 nM for 1 h) cells (30 μ g each) were subjected to immunoblot analysis using PKC α and PKC δ antibodies as shown. Details of immunoblot analysis were as described in Section 2 and figure.

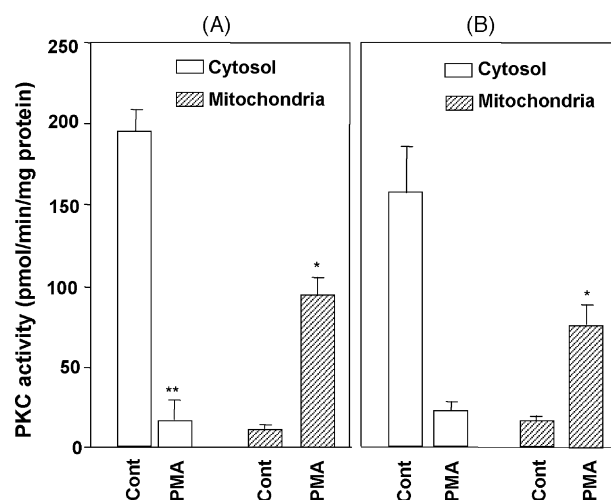


Fig. 5 – Classical and Ca²⁺ sensitive PKC activities in the cytosolic and mitochondrial fraction of PMA treated cells. C2C12 cells were treated with 100 nM PMA and PKC activity in the cytosol and mitochondria were assayed as described in Section 2. (A) PKC activity that is sensitive to pseudosubstrate inhibitor (PKC α , β , γ -specific) peptide. (B) Ca²⁺-sensitive activity assayed on the basis of inhibition by 10 mM EGTA. *Significantly different from control, $p < 0.05$; ** means highly significant $p < 0.001$. (n = 4–5 assays.)

protein (Fig. 4). In C6 glioma cells, PMA treatment did not affect the cytosolic level of PKC δ , and also no antibody stainable protein was seen in the mitochondrial fractions of either control or PMA treated cells. These results are in accordance with the observation in C2C12 myocytes that PMA induces the translocation of PKC α but not PKC δ to particulate fraction [25,26]. In COS7 cells, there was no change in the cytosolic PKC δ following PMA treatment. Interestingly, the antibody reacted with a faster migrating protein in the mitochondrial compartment of control cells which was increased three to five-fold in PMA treated cells (Fig. 4). The faster migrating component was not seen in the cytosolic fractions of either cell types. These results suggest that while there is negligible mitochondrial translocation of PKC δ in C6 glioma and C2C12 cells, a truncated PKC δ is translocated to mitochondria in COS7 cells.

3.3. Mitochondrial PKC activity in control and PMA treated cells

We ascertained if PMA induced increase of mitochondrial PKC α protein level correlates with PKC activity. The total PKC activity was measured using a specific peptide substrate and the classical PKC activity was determined using a pseudosubstrate inhibitor peptide (Fig. 5A). Ca²⁺-sensitive PKC activity was assayed based on the extent of inhibition by 10 mM EGTA (Fig. 5B). As shown in Fig. 5A and B more than 70% of the activity was Ca²⁺ dependent based on sensitivity to EGTA. Both the classical and Ca²⁺ sensitive activities were markedly reduced in the cytosolic fraction following PMA treatment, while there was a marked increase in activity in the mitochondrial fractions of C2C12 cells. Since PKC α is a Ca²⁺

sensitive enzyme, it is likely that much of the increase in mitochondrial activity was due to increased PKC α . In support of this, polyclonal antibody to PKC α effectively inhibited PMA dependent increase of mitochondrial activity (results not shown).

3.4. Increased mitochondrial PKC α causes disruption of mitochondrial membrane potential

Since mitochondrial transmembrane potential ($\Delta\psi_m$) is an important indicator of mitochondrial function *in situ*, we determined the state of mitochondrial $\Delta\psi_m$ after PMA treatment (100 nM for 1 h). We used cationic fluorescent probe MitoTracker Orange CM-H₂TM ROS (MTO) (Molecular Probes, Inc.) whose mitochondrial accumulation is directly proportional to the transmembrane potential [15]. The reduced form of the dye is taken up by actively respiring cells. Inside the cells, the dye is oxidized to mitochondrial-selective form, which sequesters inside the mitochondrial membrane matrix compartment and is converted to fluorescent form (extinction 525 nm and emission 576 nm). As shown in Fig. 6, the fluorescence units at emission 576 nm increased linearly up to 20 min in control cells. Consistent with a change in cell morphology (Fig. 2C), in PMA treated cells, there was no significant time dependent increase suggesting disrupted membrane potential. Cells treated with PMA plus PKC inhibitor GF109203X, on the other hand, showed time dependent increase in fluorescence, although at a level lower than control cells. Since the fluorescence change in these cells is reverted back to about 60% of control cells by treatment with PKC inhibitors, we conclude that PKC activity is directly involved in the collapse of $\Delta\psi_m$ in PMA treated cells. Although not shown, pretreatment with cyclosporine A had no significant protection against PMA-induced disruption of $\Delta\psi_m$. The latter results suggest that opening of permeability transition pore may be a downstream event of $\Delta\psi_m$ collapse in C2C12 myocytes.

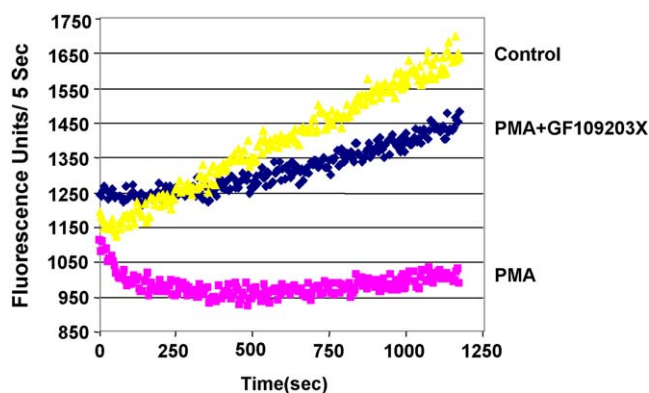


Fig. 6 – Disruption of mitochondrial membrane potential by PMA treatment. C2C12 cells were treated with (100 nM) or without PMA for 1 h in serum-free DMEM medium. In the case of PKC inhibitor GF109203X, cells were treated with 2 μ M GF109203X for 30 min before the addition of 100 nM PMA. Spectrofluorometric patterns of mitochondrial uptake of MTO (50 nM), was recorded as described in Section 2 using excitation at 525 nm and emission at 575 nm.

3.5. Effects of PMA treatment on mitochondrial respiratory chain enzyme activity and ROS production

Recent studies showed that mitochondrial cAMP activated kinase (PKA-like) modulates CcO activity [20,29]. We therefore evaluated the effect of increased mitochondrial PKC activity in PMA treated cells on the activities of mitochondrial electron transport chain complexes. PMA treatment caused significant inhibition of complex I (NADH-ubiquinone oxidoreductase activity (Fig. 7A), which was markedly reversed by pretreatment with PKC specific inhibitor GF109203X. The activities of other three complexes (complexes II, III and IV) were not significantly affected (Fig. 7B–D).

Pyruvate dehydrogenase serves as an important connecting link between glycolysis and citric acid cycle. It is well established that pyruvate dehydrogenase activity is modulated differently by glucagon and insulin through subunit phosphorylation/dephosphorylation. A kinase activity designated as PDH kinase has been implicated in glucagon-mediated inhibition of PDH activity. We therefore evaluated the effects of PMA treatment for 10–15 min on PDH activity. PDH activity was assayed by the release of ¹⁴CO₂ from [1-¹⁴C] pyruvic acid. Fig. 7E shows that PDH activity was significantly inhibited in PMA treated cells. The PMA-mediated inhibition appears to involve PKC-dependent subunit phosphorylation since PKC inhibitors GF109203X and Go6976 both reversed the PMA-mediated inhibition. These results suggest that PKC α is either directly involved in subunit phosphorylation or it activates a kinase that may be involved in subunit phosphorylation.

We determined the level of ROS production in mitochondrial isolates from control and PMA treated cells using two different assay systems. Fig. 8A shows the ROS production using the lucigenin method, which measures the O₂^{•-} (superoxide radicals). Lucigenin is known to produce non-specific signal due to redox recycling, which can be effectively controlled by using levels less than 10 μ M [20]. In support of this, Fig. 8A shows that 5 μ M lucigenin alone (or with added NADH, marked as basal activity) yielded very low signal. Swollen mitoplast with added NADH showed significant activity which could be inhibited by added superoxide dismutase (SOD) but was unaffected by catalase. This control indeed suggests that the assay method measures O₂^{•-}. Mitoplasts from cells treated with PMA for 1 h and 3 h yielded increasing levels of ROS production. Furthermore, addition of PKC inhibitor Go6850 significantly reduced the activity. The PMA-mediated ROS production was also ascertained using a more reliable DCF-DA method, which was recently modified for isolated mitochondria (Prabu K, Raza H and Avadhani N, unpublished). DCF-DA is a stable, non-fluorescent molecule, which needs to be deesterified by cellular enzyme to a form that can react with H₂O₂ and other peroxide radicals and produce fluorescence signal. As shown in Fig. 8B, DCF-DA with added NADH yielded very low signal. Mitoplasts added to the complete assay system yielded high activity which was inhibited by added catalase. Addition of SOD did not increase the signal possibly because mitochondrial SOD level is sufficient to convert O₂^{•-} to H₂O₂. The results from both of these assay methods show that PMA treatment induces mitochondrial ROS production which is effectively reversed by Go6976. We believe that the partial reversal by PKC inhibitor

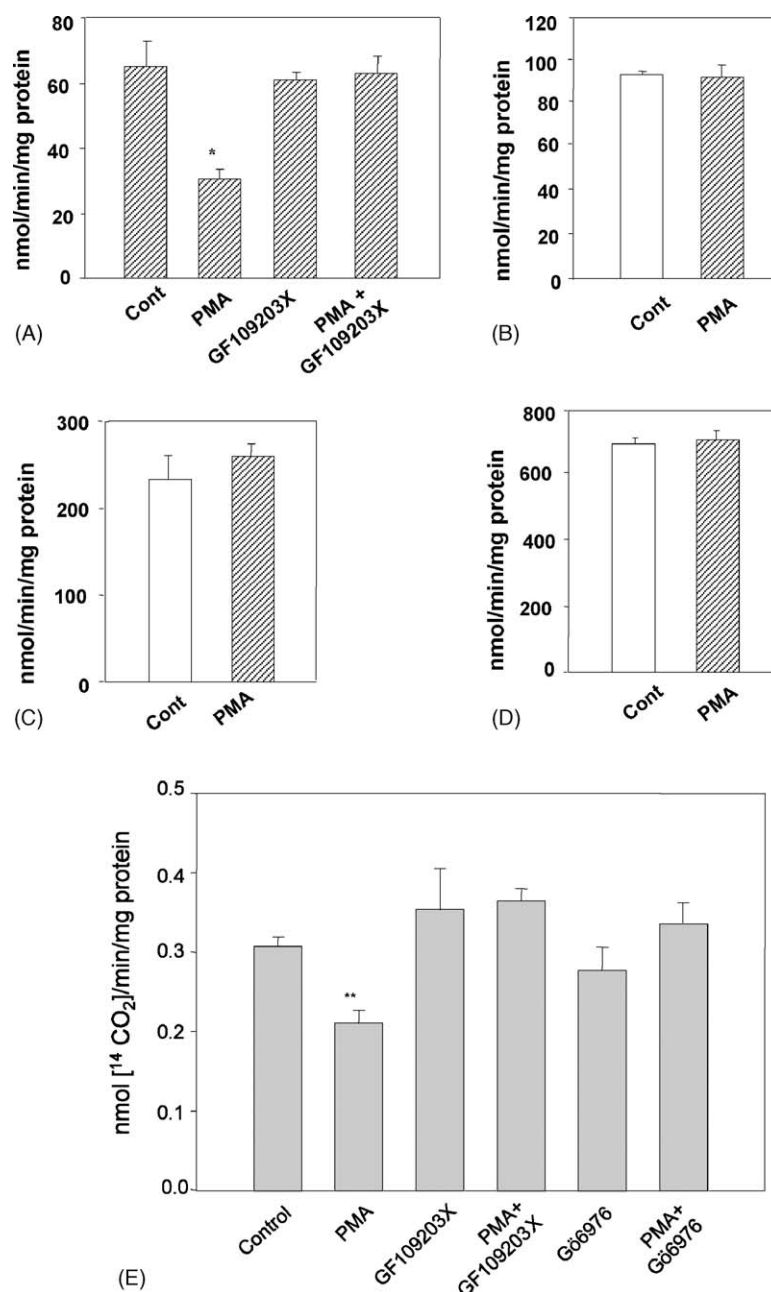


Fig. 7 – Effects of PMA treatment on the activities of mitochondrial respiratory chain complexes. Cells were incubated for 1 h in serum-free DMEM in the presence of PMA (250 nM) or DMSO as control. (A) Complex I activity, $p < 0.05$; (B) complex II activity; (C) complex II and III activity; (D) complex IV (cytochrome c oxidase) activity ($n = 5-6$); (E) PMA-induced inhibition of PDH activity in C2C12 cells. Cells were incubated in serum-free DMEM in the presence of PMA (100 nM for 1 h) or DMSO as control. Treatment with PKC inhibitor GF109203X was initiated 20 min prior to the addition of PMA. Mitochondrial isolates were assayed for PDH activity as described in Section 2. *Significantly different from control, $p < 0.001$, $n = 6$.

may be due to inefficient transport of the inhibitor into the mitochondrial compartment.

4. Discussion

In this study we show that mitochondria are the major subcellular sites for PKC α translocation in response to PMA stimulation in C2C12, C6 glioma and COS-7 cells. Although not

shown, other PKC α agonists also caused increased mitochondrial accumulation of PKC α . The mitochondrial translocated PKC α in PMA treated cells was localized in the mitochondrial innermembrane-matrix compartment causing reduced mitochondrial complex I and PDH activities, increased mitochondrial ROS production and disruption of mitochondrial transmembrane potential, $\Delta\psi_m$ (Figs. 6–8). All these changes were reversed by PKC inhibitors GF109203X, indicating the direct role of PKC α in modulating mitochondrial function. In

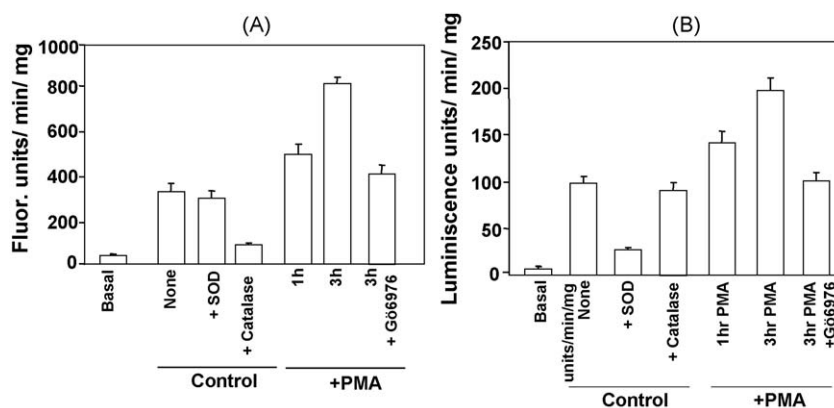


Fig. 8 – PMA-induced mitochondrial ROS production in C2C12 cells. Cells were incubated for 1 h in serum-free DMEM in the presence of PMA (100 nM) or DMSO alone as control. Treatment with PKC inhibitor GF109203X was carried out in whole cells for 20 min prior to addition of PMA or DMSO. Freshly isolated mitochondria from control and treated cells were suspended in 10 mM KH_2PO_4 buffer and used for the assay as describe in Section 2. Catalase and SOD were added to the reaction tubes before starting the reaction. Basal activity represents fluorescence or luminescence signal with the appropriate probe plus NADH. (A) Assay of peroxi radical production using the DCF-DA method. (B) Assay of O_2^- production by using the lucigenin method. $n = 4-5$.

this regard, results of this study provide mechanistic insights into PMA-induced mitochondrial injury and/or apoptosis, previously reported to occur in various cell systems [1,3,4,8,30,31].

Functional difference between various PKC isozymes and marked cell-specific differences in their response to PMA has been ascribed to the tight control of subcellular localization [26]. Among the many subtypes, PKC α (classical subtype) and PKC δ (novel subtype) are widely distributed in various tissues at relatively high abundance. PKC α largely resides in the cytosol under resting state but when cells are exposed to different stimuli the enzyme localizes to different subcellular compartments including the plasma membrane, nuclear membrane, endoplasmic reticulum and Golgi apparatus [23,24]. In this study we show that in C2C12 myoblasts, C6 glioma and COS7 cells, mitochondria are important cellular destination of PMA-mediated PKC α translocation. Recently, translocation of PKC δ by the action of different inducers such as PMA, analogs of DAG and H_2O_2 have been implicated in apoptosis. However, in C2C12 myoblasts and C6 glioma cells, we failed to detect significant PKC δ in the mitochondrial fraction following PMA treatment. The latter results are in accordance with observations in human glioma cells [25]. This may be related to the presence or absence of specific PKC binding proteins in different subcellular compartments, which may be cell and tissue specific [26].

To understand the functional or toxicological role of mitochondrial PKC α , we felt that it was important to know its precise submitochondrial location. Mitochondria contain two membranes (inner membrane and outer membrane) and two soluble compartments (intermembrane space and matrix). It is suggested that Bcl-2, an outer membrane resident protein, targets protein kinase Raf-1 to mitochondrial outer membrane, allowing this kinase to phosphorylate BAD and possibly other protein substrates involved in apoptosis [27]. PKA α catalytic subunit is localized to the inner membrane-matrix compartment following treatment with cAMP or

forskolin and the kinase is implicated in the phosphorylation of a 18 kDa subunit of complex I and three different subunits (subunits I, IV and Vb) of complex IV, CcO [21,28,29]. Present results show that both trypsin and digitonin treatment did not substantially reduce the mitochondrial PKC α level indicating that the protein subunit is located inside the inner membrane-matrix compartment. These results are consistent with immunocytochemical data in the Müller cells of the carp retina [32]. We therefore reasoned that similar to what has been shown for mitochondrial PKA, PKC α may have role in regulating the activity of mitochondrial electron transport chain complexes or mitochondrial TCA cycle enzymes.

The mitochondrial $\Delta\psi_m$ is critical for mitochondrial membrane function and oxidative phosphorylation. Some studies suggest that collapse of $\Delta\psi_m$ may have a role in the opening of PTP (mitochondrial permeability transition pore) which in turn is an important contributing factor in mitochondria-mediated pathway of apoptosis. A previous study of our laboratory showed that the mitochondrial stress signaling defined by the collapse of $\Delta\psi_m$ initiates stress signaling and causes a change in cell morphology [16,33]. Interestingly, we also observed a change in cell morphology in response to PMA-mediated disruption of $\Delta\psi_m$ (Fig. 2C). PKC inhibitor GF109203X was able to retard the PMA-induced disruption of membrane potential and change in the cell shape suggesting that PKC plays a direct role in these processes. Thus, one mechanism of PMA-induced mitochondrial dysfunction and apoptosis reported in different cell systems may involve translocation of activated PKC α into mitochondrial compartment.

PKC and PKA-mediated phosphorylation is known to regulate the function of ion channels [12,34,35]. It is also known that impaired function of mitochondrial respiratory chain complexes cause the disruption of $\Delta\psi_m$ [36,37]. Our results show a significant inhibition of complex I and PDH activity in PMA treated cells. In view of this, we postulate that disruption of mitochondrial transmembrane potential in PMA treated cells may either be due to mitochondrial PKC α -mediated inhibition

of complex I activity or altered permeability of mitochondrial ion channels. Although the precise mechanism remains unknown, inhibition of mitochondrial complex I, PDH and disruption of transmembrane potential are all reversed partly or completely by PKC inhibitors suggesting that mitochondrial PKC α plays a direct role in these processes.

Mitochondrial electron transport chain complexes (complexes I, II and IV) are important sites of ROS production [21,38,39] and mitochondrial ROS has been widely implicated in the physiological function and pathological injury. In congestive heart failure, decreased complex I enzymatic activity and impairment of electron transfer are implicated in deleterious production of ROS and resultant myocyte injury [40]. In cells subjected to hypoxia and hearts subjected to global or focal ischemia PKA-mediated subunit phosphorylation has been suggested to cause inhibition of CcO activity and increased ROS production [21]. TNF- α and interferon- γ induced ROS which cause oxidative damage to macromolecules and in contributing to tissue degeneration in target organs of autoimmune diseases [31]. Furthermore, PKC activator PMA is known to induce ROS production and apoptosis in some types of cells [31]. We propose that mitochondrial PKC α contributes substantial amount of PMA-induced ROS production.

In 3T3-L1 adipocytes, PKC α and PKC δ are implicated in PMA-stimulated glucose uptake [41]. PKC δ translocated to the mitochondrial compartment is also thought to be involved in insulin-stimulated pyruvate dehydrogenase activity [5,42,43]. In C2C12 myocytes, PKC α is the major form translocated to the mitochondrial compartment following PMA treatment. Furthermore, PKC inhibitors reverse the PMA-mediated inhibition of PDH activity. These observations lead us to conclude that PKC α plays a direct role in the modulation of PDH activity. Although the precise mechanism remains unknown, it is likely that mitochondrial PKC α may be involved in the inactivation of PDH kinase or induction of specific phosphatase.

Studies on mitochondrial proteome analysis suggest that mitochondria from unicellular eukaryotes may contain well over 1000 proteins, while those from mammalian sources may contain up to 2000 protein. More than 50% of these proteins appear to lack canonical mitochondrial targeting signals. PKC α and PKC δ belong to this latter class of proteins since both of them lack recognizable mitochondrial targeting signals. Recent studies from our laboratory showed that a number of xenobiotic inducible cytochrome P450s that are predominantly targeted to ER, cytosolic GSTs, plasma membrane targeted APP are also targeted to mitochondria by virtue of their N-terminal or C-terminal chimeric signals [13,44,45]. The cryptic mitochondrial targeting signal in these cases need to be activated either by endoproteolytic cleavage at the N-terminal sites [13] or phosphorylation of nascent chains at an internal site [45,46]. It is likely that PKA and PKCs are targeted to mitochondria through activation of chimeric signals, although the precise mechanism of activation currently remains to be elucidated.

Acknowledgements

We thank Dr. Peter M. Blumberg for providing the bovine PKC α cDNA. This research was supported by NIH grants CA-22762 and GM-49683.

REFERENCES

- [1] Parker PJ, Dekker LV. Protein Kinase C New York/Austin: Chapman & Hall/R.G. Landes Co.; 1997.
- [2] Newton AC. Protein kinase C: structure, function, and regulation. *J Biol Chem* 1995;270:28495–8.
- [3] Braiman L, Sheffi-Friedman L, Bak A, Tennenbaum T, Sampson SR. Tyrosine phosphorylation of specific protein kinase C isozymes participates in insulin stimulation of glucose transport in primary cultures of rat skeletal muscle. *Diabetes* 1999;48:1922–9.
- [4] Ohno S, Mizuno K, Adachi Y, Hata A, Akita Y, Akimoto K, et al. Activation of novel protein kinase C δ and ϵ upon mitogenic stimulation of quiescent rat 3Y1 fibroblasts. *J Biol Chem* 1994;269:17495–501.
- [5] Caruso M, Maitan MA, Bifulco G, Miele C, Vigliotta G, Oriente F, et al. Activation and mitochondrial translocation of protein kinase C δ are necessary for insulin stimulation of pyruvate dehydrogenase complex activity in muscle and liver cells. *J Biol Chem* 2002;276:45088–97.
- [6] Frevert EU, Kahn B. Protein kinase C isoforms ϵ , η , δ , ζ in murine adipocytes: expression, subcellular localization and tissue-specific regulation in insulin-resistant states. *Biochem J* 1996;316:865–71.
- [7] Noland Jr TA, Dimino MJ. Characterization and distribution of protein kinase C in ovarian tissue. *Biol Reprod* 1986;35:863–72.
- [8] Majumder PK, Pandey P, Sun X, Cheng K, Datta R, Saxena S, et al. Mitochondrial translocation of protein kinase C delta in phorbol ester-induced cytochrome c release and apoptosis. *J Biol Chem* 2000;275:21793–21796.
- [9] Li L, Lorenzo PS, Bogi K, Blumberg PM, Yuspa SH. Protein kinase C delta targets mitochondria, alters mitochondrial membrane potential, and induces apoptosis in normal and neoplastic keratinocytes when overexpressed by an adenoviral vector. *Mol Cell Biol* 1999;19:8547–58.
- [10] Baines CP, Zhang J, Wang GW, Zheng YT, Xiu JX, Cardwell EM, et al. Mitochondrial PKC epsilon and MAPK form signaling modules in the murine heart: enhanced mitochondrial PKC epsilon-MAPK interactions and differential MAPK activation in PKC epsilon-induced cardioprotection. *Circ Res* 2002;90:390–7.
- [11] Ruvolo PP, Deng X, Carr BK, May WS. A functional role for mitochondrial protein kinase C alpha in Bcl2 phosphorylation and suppression of apoptosis. *J Biol Chem* 1998;273:25436–42.
- [12] Nowak G. Protein kinase C- α and ERK1/2 mediate mitochondrial dysfunction, decreases in active Na⁺ transport, and cisplatin-induced apoptosis in renal cells. *J Biol Chem* 2002;277:43377–88.
- [13] Addya S, Anandatheerthavarada HK, Biswas G, Bhagwat SV, Mullick J, Avadhani NG. Targeting of NH₂-terminal-processed microsomal protein to mitochondria: a novel pathway for the biogenesis of hepatic mitochondrial P450MT2. *J Cell Biol* 1997;139:589–99.
- [14] Niranjana BG, Wilson NM, Jefcoate CR, Avadhani NG. Hepatic mitochondrial cytochrome P-450 system. Distinctive features of cytochrome P-450 involved in the activation of aflatoxin B1 and benzo(a)pyrene. *J Biol Chem* 1984;259:12495–501.
- [15] Szalai G, Krishnamurthy R, Hajnoczky G. Apoptosis driven by IP(3)-linked mitochondrial calcium signals. *EMBO J* 1999;18:6349–61.
- [16] Biswas G, Adebajo OA, Freedman BD, Anandatheerthavarada HK, Vijayasathya C, Zaidi M, et al. Retrograde Ca²⁺ signaling in C2C12 skeletal myocytes in response to mitochondrial genetic and metabolic stress: a

- novel mode of inter-organelle crosstalk. *EMBO J* 1999;18:522–33.
- [17] Birch-Machin MA, Turnbull DM. Assaying mitochondrial respiratory complex activity in mitochondria isolated from human cells and tissues. *Methods Cell Biol* 2001;65:97–117.
 - [18] Tisdale HD. Preparation and properties of succinic-cytochrome c reductase (complex II-III). In: Estabrook RW, Pullman ME, editors. *Methods in enzymology oxidation and phosphorylation*, vol. X. New York/London: Academic Press; 1976. p. 213–6.
 - [19] Smith L. Spectrophotometric assay of cytochrome c oxidase. In: Glick D, editor. *Methods of biochemical analysis*. New York: John Wiley & Sons; 1955. p. 427–34.
 - [20] Li Y, Zhu H, Kuppusamy P, Roubaud V, Zweier JL, Trush MA. Validation of lucigenin (bis-N-methylacridinium) as a chemiluminescent probe for detecting superoxide anion radical production by enzymatic and cellular systems. *J Biol Chem* 1998;273:2015–23.
 - [21] Prabu SK, Anandatheerthavarada HK, Raza H, Srinivasan S, Spear JF, Avadhani NG. Protein kinase A-mediated phosphorylation modulates cytochrome c oxidase function and augments hypoxia and myocardial ischemia-related injury. *J Biol Chem* 2006;281:2061–70.
 - [22] Leary SC, Battersby BJ, Hansford RG, Moyes CD. Interactions between bioenergetics and mitochondrial biogenesis. *Biochim Biophys Acta* 1998;1365:522–30.
 - [23] Björndal B, Helleland C, Lillehaug JR. Differential TPA and PDGF-BB effects on subcellular localization of PKC alpha and beta I in C3H/10T1/2 cells. *Anticancer Res* 2000;20:2633–40.
 - [24] Goodnight JA, Mischak H, Kolch W, Mushinski JF. Immunocytochemical localization of eight protein kinase C isozymes overexpressed in NIH 3T3 fibroblasts. Isoform-specific association with microfilaments, Golgi, endoplasmic reticulum and nuclear and cell membranes. *J Biol Chem* 1995;270:9991–10001.
 - [25] Besson A, Yong VW. Involvement of p21 (Waf1/Cip1) in protein kinase C alpha-induced cell cycle progression. *Mol Cell Biol* 2000;20:4580–90.
 - [26] Ron D, Kazanietz MG. New sights into the regulation of protein kinase C and novel phorbol ester receptors. *FASEB J* 1999;13:1658–76.
 - [27] Wang HG, Rapp UR, Reed JC. Bcl-2 targets the protein kinase Raf-1 to mitochondria. *Cell* 1996;87:629–38.
 - [28] Papa S, Sardanelli AM, Cocco T, Speranza F, Scacco SC, Technikova-Dobrova Z. The nuclear-encoded 18 kDa (IP) AQP subunit of bovine heart complex I is phosphorylated by the mitochondrial cAMP-dependent protein kinase. *FEBS Lett* 1996;379:299–301.
 - [29] Lee I, Salomon AR, Ficarro S, Mathes I, Lottspeich I, Grossman LI, et al. cAMP-dependent tyrosine phosphorylation of subunit I inhibits cytochrome c oxidase activity. *J Biol Chem* 2005;280:6094–100.
 - [30] Skoglund G, Hansson A, Ingelman-Sundberg M. Rapid effects of phorbol esters on isolated rat adipocytes. Relationship to the action of protein kinase C. *Eur J Biochem* 1985;148:407–12.
 - [31] Vladimirova O, Lu FM, Shawver L, Kalman B. The activation of protein kinase C induces higher production of reactive oxygen species by mononuclear cells in patients with multiple sclerosis than in controls. *Inflamm Res* 1999;48:412–6.
 - [32] Fernandez E, Cuenca N, Garcia M, De Juan J. Two types of mitochondria are evidenced by protein kinase C immunoreactivity in the Muller cells of the carp retina. *Neurosci Lett* 1995;183:202–5.
 - [33] Amuthan G, Biswas G, Anandatheerthavarada HK, Vijayasathya C, Shephard HM, Avadhani NG. Mitochondria-to-nucleus stress signaling induces phenotypic changes, tumor progression and cell invasion. *EMBO J* 2001;20:1910–20.
 - [34] Berger HA, Travis SM, Welsh MJ. Regulation of the cystic fibrosis transmembrane conductance regulator Cl⁻ channel by specific protein kinase and protein phosphorylation. *J Biol Chem* 1993;268:2037–47.
 - [35] Wang Y, Sostman A, Roman R, Stribling S, Vigna S, Hannun Y, et al. Metabolic stress opens K⁺ channels in hepatoma cells through a Ca²⁺ and protein kinase C α -dependent mechanism. *J Biol Chem* 1996;271:18107–13.
 - [36] Senoo-Matsuda N, Hartman PS, Akatsuka A, Yoshimura S, Ishii NA. Complex II defect affects mitochondrial structure, leading to ced-3 and ced-4-dependent apoptosis and aging. *J Biol Chem* 2003;278:22031–6.
 - [37] Chandel NS, Budinger GR, Choe SH, Schumacker PT. Cellular respiration during hypoxia. Role of cytochrome oxidase as the oxygen sensor in hepatocytes. *J Biol Chem* 1997;272:18808–16.
 - [38] McLennan HR, Esposti MD. The contribution of mitochondrial respiratory complexes to the production of reactive oxygen species. *J Bioenerg Biomembr* 2000;32:153–62.
 - [39] Petrosillo G, Ruggiero FM, Di Venosa N, Paradies G. Decreased complex III activity in mitochondria isolated from rat heart subjected to ischemia and reperfusion: role of reactive oxygen species and cardiolipin. *FASEB J* 2003;17:714–6.
 - [40] Ide T, Tsutsui H, Kinugawa S, Utsumi H, Kang DC, Hattori N, et al. Mitochondrial electron transport complex I is a potential source of oxygen free radicals in the failing myocardium. *Circ Res* 1999;85:357–63.
 - [41] Tsuru M, Katagiri H, Asano T, Yamada T, Ohno S, Ogihara T, et al. Role of PKC isoforms in glucose transport in 3T3-L1 adipocytes: insignificance of atypical PKC. *Am J Physiol Endocrinol Metab* 2002;283:E338–45.
 - [42] Coore HG, Denton RM, Martin BR, Randle PJ. Regulation of adipose tissue pyruvate dehydrogenase by insulin and other hormones. *Biochem J* 1971;125:115–27.
 - [43] Farese RV, Standaert ML, Barnes DE, Davis JS, Pollet RJ. Phorbol ester provokes insulin-like effects on glucose transport, amino acid uptake, and pyruvate dehydrogenase activity in BC3H-1 cultured myocytes. *Endocrinology* 1985;116:2650–5.
 - [44] Anandatheerthavarada HK, Biswas G, Robin MA, Avadhani NG. Mitochondrial targeting and a novel transmembrane arrest of Alzheimer's amyloid precursor protein impairs mitochondrial function in neuronal cells. *J Cell Biol* 2003;161:41–54.
 - [45] Robin MA, Prabu SK, Raza H, Anandatheerthavarada HK, Avadhani NG. Phosphorylation enhances mitochondrial targeting of GSTA4-4 through increased affinity for binding to cytoplasmic Hsp70. *J Biol Chem* 2003;278:18960–7.
 - [46] Anandatheerthavarada HK, Biswas G, Mullick J, Sepuri NB, Otvos L, Pain D, et al. Dual targeting of cytochrome P4502B1 to endoplasmic reticulum and mitochondria involves a novel signal activation by cyclic AMP-dependent phosphorylation at Ser128. *EMBO J* 1999;18:5494–504.